Journal of Solid State Chemistry 182 (2009) 3063–3066

Contents lists available at ScienceDirect

Journal of Solid State Chemistry

journal homepage: www.elsevier.com/locate/jssc

Synthesis, structure characterization and fluorescence property of a new fluoride borate crystal, $CdZn_2KB_2O_6F$

Zhi-Wei Jiao [a], Fan Zhang [a,b], Qing-Feng Yan [a], De-Zhong Shen [a,*], Guang-Qiu Shen [a]

[a] Department of Chemistry, Tsinghua University, Beijing 100084, PR China
[b] Enhanced Oil Recovery Department, Research Institute of Petroleum Exploration and Development, Beijing 100083, China

ARTICLE INFO

Article history:
Received 7 June 2009
Received in revised form
18 August 2009
Accepted 23 August 2009
Available online 28 August 2009

Keywords:
Fluoride borate
Crystal structure
Fluorescence

ABSTRACT

A new fluoride borate crystal, $CdZn_2KB_2O_6F$, has been synthesized by flux-supported solid-state reaction. The crystal structure has been determined by single-crystal X-ray diffraction. It crystallizes in the trigonal space group $P\overline{3}c1$ with $a=5.0381(6)$ Å, $b=5.0381(6)$ Å, $c=15.1550(19)$ Å, $\alpha=90.00^\circ$, $\beta=90.00^\circ$, $\gamma=120.00^\circ$, $Z=2$. The crystal represents a new structure type in which $ZnBO_3$ layers are connected through bridging fluorine and cadmium atoms alternately along the *c*-axis. K^+ cations are filled in the intralayer open channels to balance charge. IR and Raman spectra further confirm the crystal structure. Photoluminescent measurement reveals that $CdZn_2KB_2O_6F$ exhibits blue fluorescence at room temperature in the solid-state.

1. Introduction

Since the low temperature modification of the barium borate β-BaB_2O_4 (BBO) [1] and lithium triborate LiB_3O_5 (LBO) [2] were discovered and used for harmonic generation of laser radiation in visible and UV spectral range, there has been a rapidly growing interest in the borate system compounds. The intense studies have produced a series of new crystals with interesting optical properties, such as borates $CsLiB_6O_{10}$ (CLBO), $Gd_xY_{1-x}Ca_4O(BO_3)_3$ (GdYCOB), $Sr_2Be_2B_2O_7$ (SBBO), $K_2AlB_2O_7$ (KAB), and fluoride borates $KBe_2BO_3F_2$ (KBBF) and $BaAlBO_3F_2$ (BABF) [3–6]. Furthermore, photoluminescence is also found in many borates and some have been used as useful phosphors [7–10]. These achievements inspirit us to explore new borates with promising luminescence and optical properties.

More recently, several new borate crystals including $Cd_3Zn_3B_4O_{12}$, $CdZn_2B_2O_6$, $Cd_{1.17}Zn_{0.83}B_2O_5$, $(Cd_{0.02}Zn_{0.98})_4O(BO_2)_6$ have been found and characterized in CdO–ZnO–B_2O_3 ternary system by our group [11–14]. Among these compounds, $Cd_3Zn_3B_4O_{12}$ is the most promising nonlinear optical (NLO) material which exhibits a strong second harmonic generation (SHG) effect ($\approx$2.6KDP). However, the crystal is hard to grow because of its decomposition above melting point. To conquer this constraint, we adopted KBF_4 as a fluxing agent to grow the crystal. In this way, fluoride participation in the reaction led to a new fluoride borate $CdZn_2KB_2O_6F$. To our knowledge, it is the first fluoride borate containing both transition metals and alkali metal ions [15]. Here we describe the synthesis and structure characterization of $CdZn_2KB_2O_6F$ together with its fluorescence property.

2. Experimental section

2.1. Sample preparation

Firstly, the precursor $Cd_3Zn_3B_4O_{12}$ was synthesized according to the procedure described previously [14], using solid-state reactions of stoichiometric amounts of CdO (99.8%), ZnO (99.95%) and H_3BO_3 (99.99%). Then, mixture of appropriate quantities $Cd_3Zn_3B_4O_{12}$ and KBF_4 (99.0%) were ground to a fine powder in a mortar and compressed into a Pt crucible. The mixture was gradually heated to 800 °C, keeping at this temperature for one day for complete melting. The melt was cooled down to 700 °C at a rate of 1 °C/h, followed by cooling to room temperature at 20 °C/h. Colorless crystals with millimeter grade could be seen in the solidified melt. They were then isolated mechanically for further test. It should be noted that, if the temperature is above 900 °C in the reaction process, the aimed product would not be obtained.

2.2. X-ray crystallography

Powder X-ray diffraction analysis of as-grown crystals was performed on a Brüker D8 Advance diffractometer with steps of $0.020^\circ(2\theta)$ using the Cu$K\alpha$ radiation at room temperature. The angle range was taken from $2\theta=10^\circ$ to 70° in the continuous scan

---

[*] Corresponding author. Fax: +86 10 62771149.
E-mail address: jzwzwj@163.com (D.-Z. Shen).

0022-4596/$ - see front matter © 2009 Elsevier Inc. All rights reserved.
doi:10.1016/j.jssc.2009.08.020

mode. No analogue of the X-ray powder diffraction pattern was found in the powder diffraction file database (Fig. 1).

Single-crystal X-ray diffraction measurement was carried out on a Brüker Smart-1000 CCD diffractometer using Mo $K\alpha$ radiation (λ=0.71073 Å). The structure was solved by direct methods and expanded using Fourier difference map with SHELXL-97 program package [16]. The crystallographic data, the details of X-ray data collections, and refinement parameters for the structure determination are presented in Table 1. The final atomic coordinates with equivalent isotropic displacements for $CdZn_2KB_2O_6F$ are given in Table S1. Selected bond distances and angles are in Table S2.

2.3. Physical measurements

The concentrations of Cd^{2+}, Zn^{2+}, K^{+} and B^{3+} in the crystal were determined using an ICP-AES spectrometer, and the results are listed in Table S3. ^{19}F NMR spectra were taken on a Bruker AV-400 spectrometer operating at 400 MHz. The melting behaviors of the crystal were investigated by differential thermal analysis (DTA) performed on a Shimadzu DTA-50 differential thermal analyzer in air at a heating rate of 20 °C/min. Infrared spectra were recorded using the FT-IR PE Spectrum GX spectrometer in the range from 400 to 4000 cm^{-1} at 4 cm^{-1} resolution using KBr pellet. Raman spectra were collected from 200 to 2000 cm^{-1} using an RM 2000 microscopic confocal Raman spectrometer (Renishaw PLC, England) with a backscattering configuration, and the excitation laser was irradiated from an Ar^{+} laser with the wavelength of 633 nm. The luminescent spectra for the powdered solid sample were recorded at room temperature on an LS-55 spectrofluorometer with a xenon arc lamp as the light source. The pass width is 0.5 nm in the measurements of emission and excitation spectra.

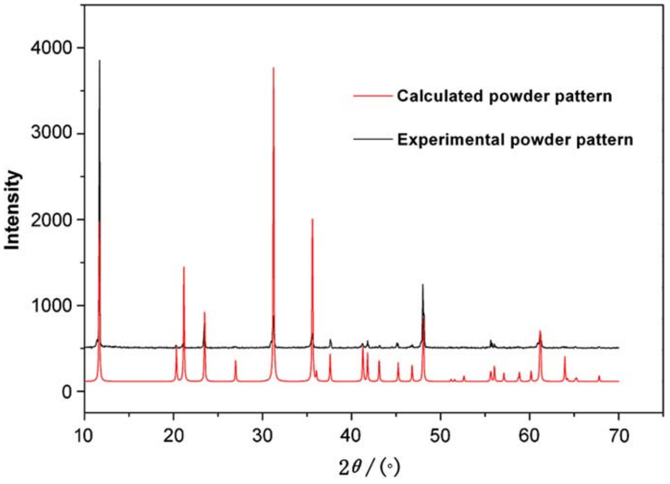

Fig. 1. Comparison of experimental and the calculated X-ray powder diffraction patterns of $CdZn_2KB_2O_6F$.

Table 1
Crystallographic data and structure refinement parameters for $CdZn_2KB_2O_6F$.

Crystal	$CdZn_2KB_2O_6F$
Crystal system	Trigonal
Space group	$P\overline{3}c1$ (No.165)
a	5.0381(6) Å
b	5.0381(6) Å
c	15.1550(19) Å
α	90.00°
β	90.00°
γ	120.00°
V	333.13(7) $Å^3$
Z	2
Formula weight	418.86
Temperature	295(2) K
Wavelength	0.71073 Å
Calculated density	4.176 g/cm^3
Absorption coefficient	10.932 mm^{-1}
F(000)	388
Refinement method	Full-matrix least-squares on F^2
Goodness-of-fit on F^2	1.034
Crystal size	0.14 × 0.1 × 0.1 mm^3
Theta range for data collection	2.69°–37.48°
Total reflections/unique (R_{int})	2534/599 (0.0191)
Limiting indices	$-8 \le h \le 8$, $-8 \le k \le 8$, $-25 \le l \le 25$
Final R indices [$I > 2\sigma(I)$]	R_1=0.0374, wR_2=0.0816
R indices (all data)	R_1=0.0400, wR_2=0.0829
Extinction coefficient	0.0201(17)
Largest diff. peak and hole	1.547 and −2.288 $Å^{-3}$

3. Results and discussion

3.1. Reaction discussion

It is noteworthy that KBF_4 not only takes part in the reaction, but also serves as a flux agent in the reaction. So excess of KBF_4 is necessary in the experiment.

The structure of $Cd_3Zn_3B_4O_{12}$ plays a key role in the formation of $CdZn_2KB_2O_6F$. $Cd_3Zn_3B_4O_{12}$ crystallizes in the noncentrosymmetric space group $R3c$ and is characterized by a three-dimensional framework built from corner-sharing BO_3 triangles with CdO_4 or ZnO_4 tetrahedra. The Cd^{2+} and Zn^{2+} cations share the same site and are disordered [11]. According to the Theory of Hard and Soft Acids and Bases (HSAB) [17,18], Cd^{2+} belongs to the soft acid and Zn^{2+} belongs to the intermediate acid. So while the fluoride is introduced into the reaction system, it tends to interact with the Zn^{2+} rather than Cd^{2+}. This effect results in the Zn^{2+} and Cd^{2+} no longer occupying on the same site and allows Cd^{2+} to adopt regular octahedral coordination geometry. In this way, the inversion centers are created and the structure transforms to the centrosymmetric space group $P\overline{3}c1$ of the title crystal (Fig. 2). The effect of fluorine in the reaction indicates that fluorine could

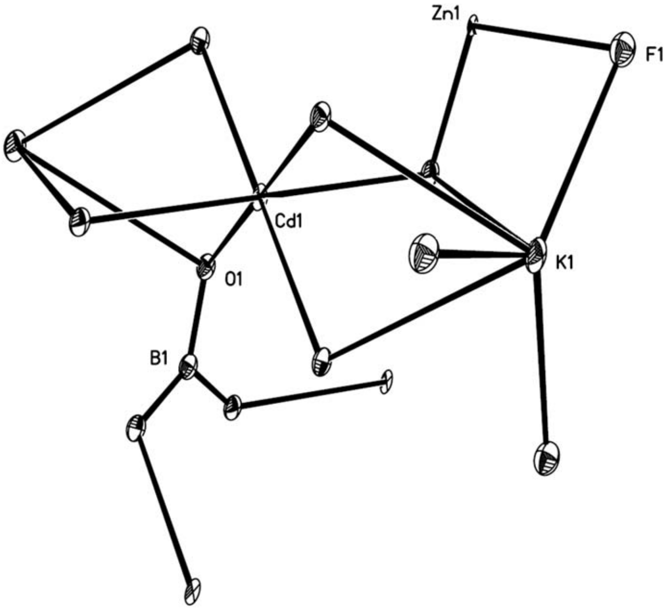

Fig. 2. The ORTEP structure of $CdZn_2KB_2O_6F$ (50% probability thermal ellipsoids) showing the unique atoms.

be probably introduced to react with the borates of mixed metal systems to explore new fluoride borate compounds.

3.2. *Crystal structure description*

The structure of $CdZn_2KB_2O_6F$ is depicted in Fig. 3. It consists of K^+ ions, BO_3 triangles, CdO_6 octahedra and ZnO_3F tetrahedra. $CdZn_2KB_2O_6F$ represents a new structure type among the few known fluoride borates. In this configuration, all the BO_3 trigonal groups are perpendicular to the *c*-axis with the B–O bonds sharing the same length 1.382(2) Å. The sum of the three O–B–O angles is equal to 120° which indicates that the BO_3 trigonal group is perfectly planar.

Zn atom is coordinated by three O atoms and one F atom with the bond length of 1.933(1) and 2.023(1) Å respectively, to form a distorted ZnO_3F tetrahedron. The BO_3 triangles and ZnO_3 of ZnO_3F tetrahedra form an infinite $ZnBO_3$ layer through sharing bridging O atoms with each other as shown in Fig. 4. All the atoms in the layer are nearly in the same plane except the Zn atoms slightly deviating from it due to their bonds to the F atoms. The layers here are similar with the layers in $Sr_2Be_2B_2O_7$ (SBBO), $KBe_2BO_3F_2$ (KBBF) and $BaAlBO_3F_2$ (BABF) [4]. But unlike the latter crystals, a series of cadmium and bridging fluorine atoms link the adjacent $ZnBO_3$ layers alternately to form a unique three-dimensional framework as shown in Fig. 5. Each CdO_6 octahedron shares three O atoms with one $ZnBO_3$ layer and the other three with another adjacent layer. All the Cd–O bonds in the CdO_6 octahedra share the same length 2.297(3) Å comparable to the Cd–O bonds in $Cd_3(BO_3)_2$ [19]. The Cd^{2+} cation is characterized by a typical and nearly regular octahedral geometry.

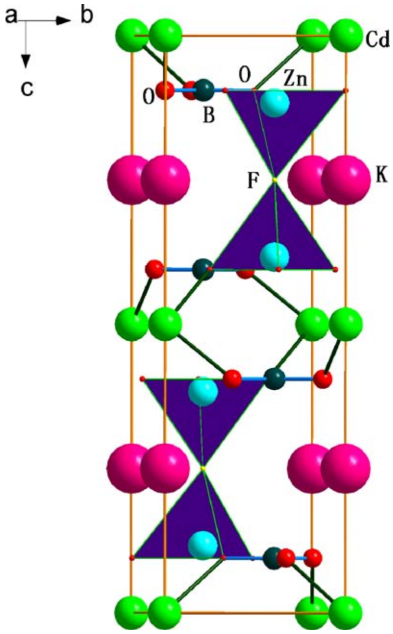

Fig. 3. The refined structure of $CdZn_2KB_2O_6F$.

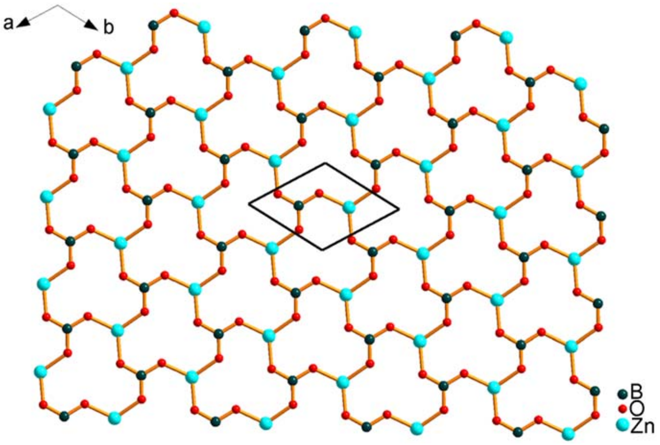

Fig. 4. The single $ZnBO_3$ layer.

K^+ ions are filled in the channels along [010] or [100] direction. Each K^+ ion is surrounded by six O atoms and three F atoms with the length of 2.954(3) Å (K–O) and 2.909(0) Å (K–F), respectively. Bond valence sum (BVS) value of 0.905 for K^+ ion shows that it is in agreement with its expected formal valence [20,21].

3.3. *Differential thermal analysis*

The differential thermal analysis of $CdZn_2KB_2O_6F$ is shown in Fig. 6. A sharp endothermal peak at 861 °C associated with its melting point. But a continuous endothermal process immediately appears above the melting point corresponding to a considerable weight loss process as shown in the TG curve, which indicates that a decomposition reaction probably occurred and some reaction products volatilized at high temperature.

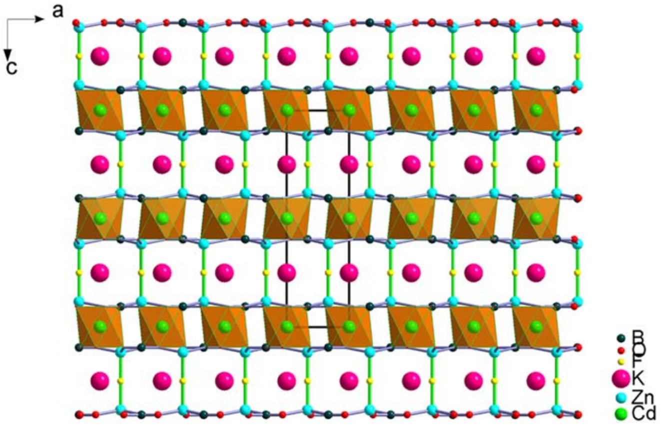

Fig. 5. The crystal structure of $CdZn_2KB_2O_6F$ projected along the *b*-axis with CdO_6 octahedron and K^+ ions filling in the channels.

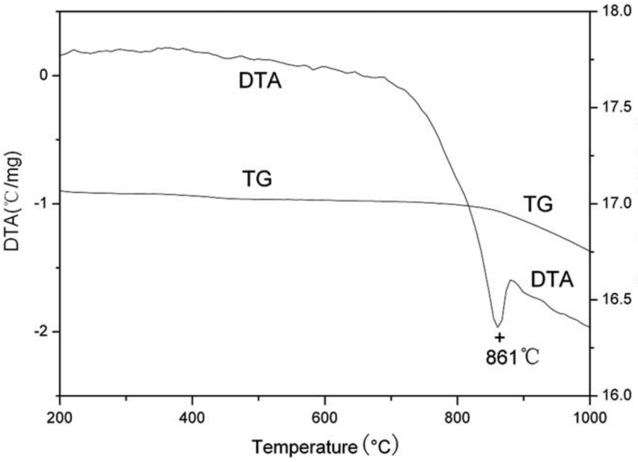

Fig. 6. DTA and TG curves of $CdZn_2KB_2O_6F$.

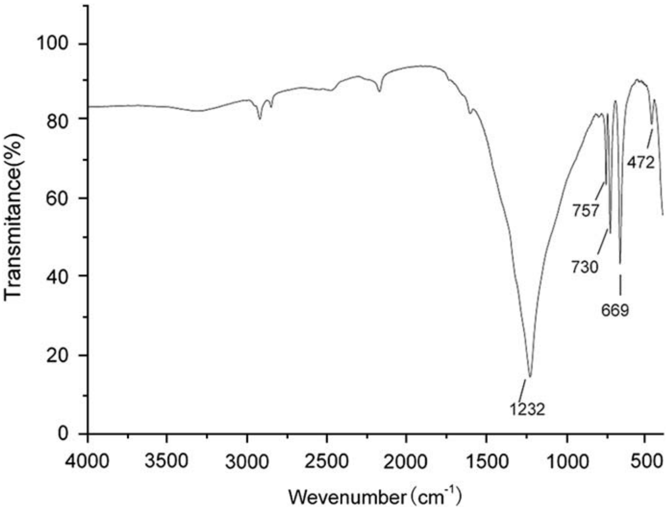

Fig. 7. Infrared spectra of $CdZn_2KB_2O_6F$.

3.4. IR and Raman spectra

Fig. 7 shows the complete spectral region of the IR spectra between 400 and 4000 cm^{-1}. The strong bands near 1232 cm^{-1} arise from BO_3 antisymmetric stretching vibrations and those between 600 and 800 cm^{-1} characterize the bending modes of triangular BO_3 groups, which further confirm the existence of trigonally coordinated boron atoms. The absorption peaks near 450 cm^{-1} are due to the ZnO_4 groups [22,23]. In the Raman spectra (Fig. S1), the peaks between 665 and 945 cm^{-1} can be assigned to the absorption of BO_3 groups. The absorption peaks of ZnO_3F and CdO_6 groups are located below 450 cm^{-1} [22].

3.5. Fluorescence property

In the Ref. [24], it was indicated that the pure $CdZn_2B_2O_6$ was not luminescent without activators. But simple $CdZn_2KB_2O_6F$ powder exhibited distinct blue photoluminescence with the emission peaks at 471 and 483 nm on the excitation at 389 and 400 nm, respectively (Fig. S2 and S3). Considering the unique structure of title compound, its fluorescence behavior may be attributed to the planar sandwich layers coordinated to the Cd^{2+} ions. And charge transfer may takes place between the Cd^{2+} ions and the $ZnBO_3$ layers.

4. Conclusion

In summary, a novel fluoride borate $CdZn_2KB_2O_6F$ has been synthesized, and the crystal structure has been determined by single-crystal X-ray diffraction method. It is a layer-type structure and the $ZnBO_3$ layers are connected through cadmium and bridging fluorine atoms alternately. The effect of the fluorine in the reaction provokes us to explore new fluoride borate crystals. IR and Raman spectra have been investigated to confirm the crystal structure. DTA results indicate that the crystal tends to decompose above the melting point. The solid-state fluorescent measurement reveals that the compound exhibits blue fluorescence at room temperature.

Acknowledgments

This work was financially supported by the National Natural Science Foundation of China (NSFC) under the Grant no. 50590402.

Appendix A. Supplementary material

Supplementary data associated with this article can be found in the online version at doi:10.1016/j.jssc.2009.08.020.

References

[1] C.T. Chen, B. Wu, A. Jiang, G. You, Sci. China B. 18 (1985) 235–243.
[2] C.T. Chen, Y. Wu, A. Jiang, G. You, R. Li, S. Lin, J. Opt. Soc. Am. B 6 (1989) 616–621.
[3] T. Sasaki, Y. Mori, M. Yoshimura, Y.K. Yap, T. Kamimura, Mater. Sci. Eng. R 30 (2000) 1–54.
[4] P. Becker, Adv. Mater. 10 (1998) 979–991.
[5] H. Zhang, G. Wang, L. Guo, A. Geng, Y. Bo, D. Cui, Z. Xu, R. Li, Y. Zhu, X. Wang, C. Chen, Appl. Phys. B 93 (2008) 323–326.
[6] M. Yoshimura, Y. Mori, Z.G. Hu, T. Sasaki, Opt. Mater. 26 (2004) 421–423.
[7] Z.W. Pei, Q. Su, J.Y. Zhang, J. Alloys Compds. 198 (1993) 51–53.
[8] A. Diaz, D.A. Keszler, Chem. Mater. 9 (1997) 2071–2077.
[9] R. Sankar, Solid State Sci. 10 (2008) 1864–1874.
[10] C.J. Duan, W.F. Li, J.L. Yuan, J.T. Zhao, J. Alloys Compds. 458 (2008) 536–541.
[11] T.Q. Sun, F. Pan, R.J. Wang, G.Q. Shen, X.Q. Wang, D.Z. Shen, Acta Cryst. C 59 (2003) 107–108.
[12] F. Zhang, D.Z. Shen, G.Q. Shen, Chin. Phys. Lett. 25 (2008) 1301–1304.
[13] X. Yuan, D.Z. Shen, X.Q. Wang, G.Q. Shen, J. Cryst. Growth 292 (2006) 463–485.
[14] F. Zhang, D.Z. Shen, G.Q. Shen, X.Q. Wang, Mater. Res. Bull. 43 (2008) 3188–3194.
[15] H. Park, J. Barbier, J. Solid State Chem. 155 (2000) 354–358.
[16] G.M. Sheldrick, SHELXL-97, Program for Crystal Structure Refinement, University of Göttingen, Göttingen, Germany, 1997.
[17] R.G. Pearson, J. Am. Chem. Soc. 85 (1963) 3533–3539.
[18] R.G. Parr, R.G. Pearson, J. Am. Chem. Soc. 105 (1983) 7512–7516.
[19] Y.H. Zhao, X.A. Chen, X.A. Chang, J.L. Zuo, M. Li, Acta Cryst. E 63 (2007) 50–52.
[20] N.E. Brese, M.O. Keeffe, Acta Cryst. B 47 (1991) 192–197.
[21] A. Filaretov, K.J. Schenk, D. Rusakov, G. Chapuis, Acta Cryst. C 63 (2007) 54–56.
[22] K. Nakamoto, Infared and Raman Specture of Inorganic and Coordination Compounds, fourth ed., Wiley, New York, 1986.
[23] A. Haberer, H. Huppertz, J. Solid State Chem. 182 (2009) 888–895.
[24] D.E. Harrison, F.A. Hummel, J. Electrochem. Soc. 106 (1959) 24–26.